

Optimized guided mode resonant structure as thermo-optic sensor and liquid crystal tunable filter

I. Abdulhalim

Department of Electrooptic Engineering, Ben Gurion University of the Negev, Beer Sheva 84105, Israel

E-mail: abdulhlm@bgu.ac.il

Received February 12, 2009

Applicability of guided mode resonant structures to tunable optical filtering and sensing is demonstrated using nematic liquid crystals. As a sensor, a minimum refractive index detectivity of 10^{-5} is demonstrated while as a tunable filter, tunability range of few tens of nanometers with 2-nm bandwidth is presented. The optimum design is achieved by maximizing the evanescent field region in the analyte which maximizes the overlap integral. The device can be operated in reflection or transmission modes at normal incidence. It can also be operated at a single wavelength by measuring the angular profile of the light beam.

OCIS codes: 050.5745, 050.6624, 130.2790, 230.3720.

doi: 10.3788/COL20090708.0667.

Subwavelength and nanophotonic structures exhibit wide variety of optical effects that make them useful for applications in switching, sensing, modulation, and tunable filtering. Particularly when these structures are periodic such as a grating type structure, several extraordinary novel phenomena arise, for example, the anomalous resonant transmission through metallic nano slits, the localized surface plasmon resonance near metallic sharp edges and nano particles, the guided wave resonance in sub-wavelength gratings, the negative refraction, and the polarization conversion properties over a wide range. Scatterometric and resonant grating based type sensors were theoretically investigated recently^[1] exhibiting high sensitivity to refractive index variations thus having a great potential as biosensors. When a material with variable refractive index is in contact with these structures, their optical properties are modified due to the interaction with the evanescent optical field and this can be used for sensing and modulation of light. The subject of sharp resonances in the diffraction efficiency of diffraction gratings can be traced back to 1902^[2]. Distinction between the resonant and nonresonant anomalies was first proposed in 1941 by Fano^[3] who found that the former was because of the excitation of guided waves and the latter appeared when some diffraction order is being passed off. In 1965, Hessel *et al.* proposed a phenomenological approach to resonant anomalies that introduced the poles and zeros of the diffraction efficiency^[4]. The pole appears because of guided-wave excitation which is a result of the solution of the homogeneous problem when a guided wave exists without an incident wave. The phenomenological approach (as well as grating anomalies, in general) has been the subject of extensive studies. Several researchers described this approach and showed how to use the results for predicting the behavior of anomalies^[5,6]. Recently the subject was connected with dielectric-grating anomalies because of the potential applications of such gratings as narrow-band optical filters^[7-10]. In brief, when a waveguide mode is excited in a dielectric grating (usually a corrugated waveguide), the pole leads to a peak and the zero to a dip in the diffraction efficiency and, in particular, in the reflectivity and the transmittivity of the

device. A cavity is formed for the diffracted order and a reflection resonance is obtained when the phase difference between the transmitted and reflected waves is multiples of π ^[11,12]. When the overall (non resonant) reflectivity is low, the high (theoretically 100%) and narrow peak in the reflectivity can be used for sensing^[13-15] or spectral filtering^[16,17]. Since the propagation constants of the guided wave are polarization dependent, the position of the peak depends strongly on the polarization; thus the filtering properties are polarization selective. Some experimental results verifying the theoretically predicted high resonant efficiencies for reflection filters have also been reported from the millimeter wave region to the visible region^[8,18-20]. Recently tunable filtering was demonstrated electromechanically^[21,22] and using liquid crystals both by optically^[23] and electrically^[24,25] tuning the effective index, however, the electrical tuning showed small tuning range. In this letter, we report a sensor and tunable filter based on a subwavelength grating guided wave resonant structure, which exhibits large tuning range up to 80 nm both electrically and thermally using liquid crystal material in the nematic phase. The thermal tuning is of particular interest as it demonstrates the thermal sensing ability of this device.

The reflected resonant peak shape was shown by Neviere *et al.*^[26] to be a Lorentzian. The angular shape of the peak can be written as

$$R_A = \frac{|\kappa_a|^2/k^2}{(\sin \theta - \sin \theta_{\text{peak}})^2 + (\Gamma/k)^2}, \quad (1)$$

where κ_a represents a coupling constant, Γ is a loss parameter, θ is the incidence angle in air. The peak location is determined from $\sin \theta_{\text{peak}} = n_{\text{eff}} - m\lambda/\Lambda$, where n_{eff} is the effective refractive index, m is the diffraction order, Λ is the grating period, and the width at the half maximum is $\Delta\theta = (180/\pi) [\lambda\Gamma/(\pi\cos \theta_{\text{peak}})]$. The spectral shape can be written as

$$R_s = \frac{|\kappa_w|^2 (\Lambda\lambda_{\text{peak}}/2\pi)^2}{(\lambda - \lambda_{\text{peak}})^2 + \lambda^2(\Lambda\Gamma/2\pi)^2}, \quad (2)$$

where the peak wavelength λ_{peak} is determined as

$(n_{\text{eff}} - \sin\theta)\Lambda/m$, and the spectral width $\Delta\lambda$ is given by $(\lambda_{\text{peak}}\Delta\Gamma/\pi)$. Note that $R_s = 1$ when $\kappa_a = \kappa_w = \Gamma$.

The basic parameters for the design of the guided mode resonance (GMR) structure can be determined from Eqs. (1) and (2), particularly the peak position, shape, and width. The effective index should be determined from the mode dispersion relation similar to a multilayer waveguide (WG) problem. Since usually the grating layer is much thinner than a wavelength, it can be ignored and the results in this approach are obtained in good approximation. These approaches can give the resonance spectrum including absorption, exact value of the peak width, and its dependence on the grating parameters. A less heavy approach uses the characteristic matrix approach where the grating layer is homogenized to a uniaxial thin film within the effective medium approximations. The 4×4 matrix approach^[27] can handle anisotropic layers as it is used recently^[28] to show that the effective mode index calculated in this way agrees very well with the rigorous approaches. In order to maximize the peak reflectivity, the grating period should be less than the wavelength so that only the zero order is supported and the first diffraction order exists in the WG ($m = 1$). The existence of higher modes will pull the energy away from the supposed orders. Losses are the results of absorption and scattering due to defects particularly in the WG layer, where the interaction region is large and due to imperfect collimation of the incident light beam. As a sensor, the WG index and thickness should be chosen to make the evanescent field extend more in the analyte region. In order to reduce the background reflection outside the resonance region, the layers should be carefully designed and perhaps might use the anti-reflection coating (ARC) between them. As it is difficult to implement optimization by the rigorous approach due to the heavy numerical calculation, it can be done with thin film design software or the use of the characteristic matrix approach with the grating film homogenized to the uniform uniaxial film. Fine tuning of the structure parameters can then be done with the rigorous calculation.

The basic structure of the device is shown in Fig. 1, where the grating layer is on the top of the waveguide layer and the analyte material is covering the grating that can in principle fill both the spaces between the grating lines and the space above the gratings. The basic driving design concept is based^[29] on the fact that with any evanescent wave sensing the sensitivity and hence tuning range are maximized when the overlap integral is maximized:

$$\delta k \approx -\frac{k_i V_{\text{in}}}{2} \frac{\int \delta \varepsilon E_i^* \cdot E_f dr}{\int \varepsilon E_i^* \cdot E_i dr}, \quad (3)$$

where δk is the shift in the k -vector (or effective index) of the guided mode due to a change in the analyte dielectric constant from ε to $\varepsilon + \delta\varepsilon$; E_i and k_i are the field and its wavevector before the variation took place in the analyte index, while E_f is the field after the index perturbation. The overlap integral is proportional to the interaction volume V_{in} , which depends on the evanescent field decay region. Hence if the structure is designed to make the evanescence region extend deeper into the analyte re-

gion [liquid crystal (LC) in our case], the sensitivity and therefore the tuning range are enhanced. The evanescence region is determined by the waveguide thickness and the difference between its refractive index and the LC refractive index. Hence to obtain larger tuning range, one should use high index LC material to maximize the evanescence region, and it should have high birefringence to get the large index tuning with the voltage.

The waveguide layer is made of Si_3N_4 while the grating is made of SiO_2 and Si_3N_4 lines prepared on the top of a Si substrate which is oxidized with a $2\text{-}\mu\text{m}$ layer to act as cladding for the waveguide. The Si substrate is coated on the external surface with thin dielectric layers as ARCs. For tunable filtering, a LC $2\text{-}\mu\text{m}$ -thick layer sandwiched between the top of the grating and an indium tin oxide (ITO) coated glass slide treated with a polymer alignment layer. The uniform gap was achieved using silica microspheres mixed with ultraviolet (UV) glue (Norland 68) and placed near the corners of the substrates. A special mechanical jig is used to assemble the two substrates together while observing the reflected interference fringes using a green lamp. Once a uniform green color was obtained, a UV light was shined to cure the silica spheres embedded in the glue. The LC material used is E44 from Merck that has the refractive indices of $n_{\perp} = 1.506$ and $n_{\parallel} = 1.726$ in the spectral range from 1500 to 1600 nm, which are nearly constants in this spectral range^[30]. The LC layer was tuned by applying a 100-kHz square wave voltage. The grating pitch, refractive indices, height, and fill factor are $\Lambda = 920$ nm, $n_H = 1.95$, $n_L = 1.44$, $d_g = 150$ nm, and $f = 0.5$, respectively. For the design of the structure, we calculated the mode effective index using the analytic 4×4 matrix approach^[27], which agrees very well with the rigorous coupled wave approach^[28].

In Fig. 2, measured reflection and transmission spectra of TM-polarized waves at different voltages covering the spectral range from 1530 to 1576 nm are presented exhibiting full-width at half-maximum (FWHM) of 1.5–2 nm. The voltage causes rotation of the molecules

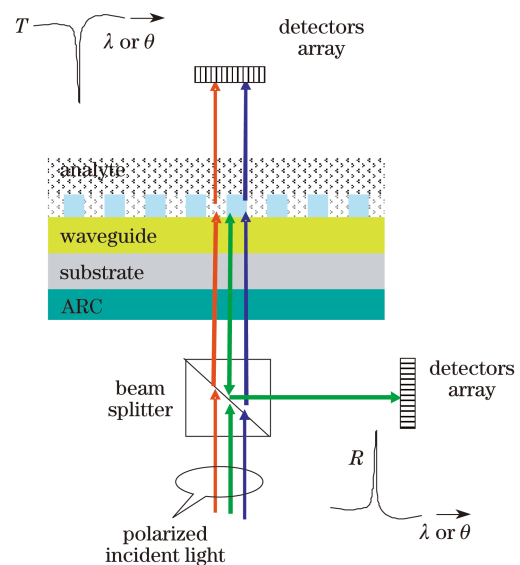


Fig. 1. Schematic of the grating guided mode resonant structure and the experimental setup.

towards the normal to the plates hence decreasing the tilt angle of the molecules which in turn causes variation in the effective index. The resonance wavelength at normal incidence is $\lambda_{\text{peak}} = \Lambda n_{\text{eff}}$, hence for $\Lambda = 920$ nm, the wavelengths fall within the optical telecommunication window. Tunability range of the filter can be increased by using LC materials with high birefringence. In our case, the sensitivity of the device is of the order of $\partial\lambda_{\text{peak}}/\partial n_{\text{eff}} \approx 200$ nm/RIU, hence with the resolution of $\delta\lambda = 2$ pm, one can obtain refractive index detectivity of $\delta n = \delta\lambda/(\partial\lambda_{\text{peak}}/\partial n_{\text{eff}}) = 10^{-5}$ RIU. The determination of the peak location with such high precision is possible if the system has high signal-to-noise ratio and also using signal processing approaches to find the peak location with subpixel resolution as it was demonstrated recently on surface plasmon resonance sensors^[31].

Another potential application of the LC layer within the structure is for temperature sensing or alternatively tunable filtering with temperature because the LCs have high thermo-optic coefficient in particular near the phase transition to the isotropic liquid phase. It can be shown that near the transition the temperature sensitivity is of the order of 10 nm/°C, hence sensitivity to 0.1 mdeg. can be obtained because $\partial\lambda_{\text{peak}}/\partial T = \Lambda\partial n_{\text{eff}}/\partial T$ and $\partial n_{\text{eff}}/\partial T$ becomes as large as 0.06 RIU/°C near the phase transition^[32] thus giving tuning of the wavelength by few tens of nm. One can then design a remote temperature sensor using an optical fiber with the guided wave sensor deposited on its distal end. In order to demonstrate

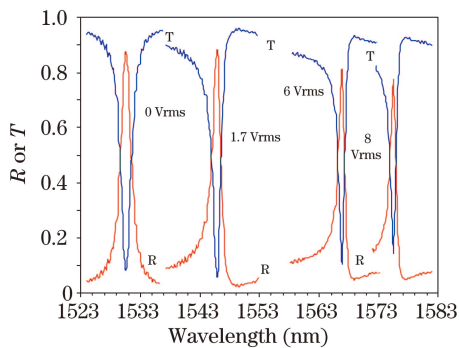


Fig. 2. Measured reflection and transmission spectra from guide mode resonant structure demonstrating tunability of the resonance as a peak in reflection or dip in transmission.

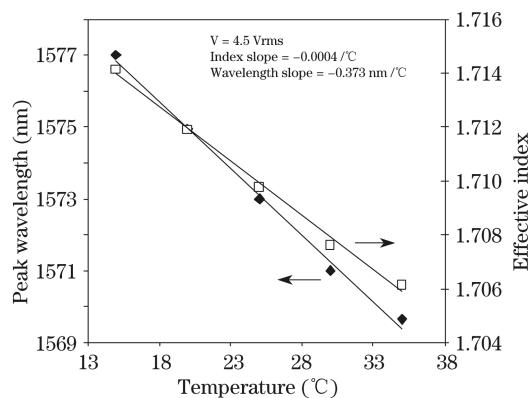


Fig. 3. Demonstration of the device as a temperature sensor showing both the refractive index sensitivity and the peak wavelength sensitivity.

this action, the device is held on a thermoelectric cooler which can allow heating and cooling between -5 and 110 °C. In Fig. 3, tunability of the peak wavelength with temperature is shown together with the effective index variations showing large sensitivity exhibiting a slope of 0.374 nm/°C near room temperature. However, the phase transition temperature of this LC to the isotropic phase is 101 °C, hence near that temperature, we expect higher thermal sensitivity and tunability by at least a factor of 10. Relatively large voltage is used in order to maximize the sensitivity to temperature because the effective index of the waveguide increases with the voltage^[28].

There are several attractive properties of the device to be used both as a narrow filter and as a sensor: 1) planar geometry; 2) made of standard dielectric materials; 3) can be manufactured easily in mass production with Si fabrication technology on the wafer scale and used for multi-sensing functionality; 4) can be operated at normal incidence; 5) exhibits large sensitivity, at least comparable to the sensitivity of the planar WG sensor and; 6) can be operated both in spectral mode and in angular mode. In the angular mode, a single wavelength is used and a beam exhibits a spread of angles, for example the natural spread from a laser diode. The centroid of the beam is detected using an array of detectors such as a charge coupled device (CCD) camera. Any shift in the reflection resonant angle will affect the centroid of the beam. In the spectral mode, a collimated beam is used containing a relatively wide spectral range and the spectrum is analyzed using a spectrometer. Alternatively, a tunable source can be used for continuous scanning of the wavelength and a single pixel detector.

In conclusion, among the sensors based on the resonant guided wave structures, the grating coupled resonant structure is one of the most attractive ones as it allows normal incidence operation in spectral or angular modes with high sensitivity. The resonance can be observed as a peak in the reflectivity either observed at fixed incidence angle versus wavelength or at fixed wavelength versus angle. It is shown that the design follows the same rules as for planar waveguide structures and the use of the characteristic matrix is proposed as a powerful tool when multilayered structures are involved. With the grating homogenized as a uniaxial plate, the use of the 4×4 matrix approach is necessary instead of the 2×2 matrix method, where the mode effective indices are determined as the poles of the reflectivity function. The structure proposed has the potential of being used in multi-arrays as a biochip using standard Si technology as well as a tunable filter when combined with LCs.

This work was supported by the Ministry of Science under Tashtiot Project. Part of the work was initiated when the author was in GWS-Photonics Inc.

References

1. I. Abdulhalim, M. Auslender, and S. Hava, *J. Nanophoton.* **1**, 011680 (2007).
2. R. Wood, *Philos. Mag.* **4**, 396 (1902).
3. U. Fano, *J. Opt. Soc. Am. A* **31**, 213 (1941).
4. A. Hessel and A. A. Oliner, *Appl. Opt.* **4**, 1275 (1965).
5. M. Neviere, in *Electromagnetic Theory of Gratings*, R. Petit, (ed.) (Springer-Verlag, Berlin, 1980) Chap. 5.

6. E. Popov, in *Progress in Optics* Vol. XXXI, E. Wolf, (ed.) (Elsevier, Amsterdam, 1993) pp. 139–187.
7. A. Sharon, D. Rosenblatt, A. A. Friesem, H. G. Weber, H. Engel, and R. Steingrueber, *Opt. Lett.* **21**, 1564 (1996).
8. A. Sharon, D. Rosenblatt, and A. A. Friesem, *J. Opt. Soc. Am. A* **14**, 2985 (1997).
9. N. Destouches, J.-C. Pommier, O. Parriaux, T. Clausnitzer, N. Lyndin, and S. Tonchev, *Opt. Express* **14**, 12613 (2006).
10. S. M. Norton, G. M. Morris, and T. Erdogan, *J. Opt. Soc. Am. A* **15**, 464 (1998).
11. D. Rosenblatt, A. Sharon, and A. A. Friesem, *IEEE J. Quantum Electron.* **33**, 2038 (1997).
12. S. Glasberg, A. Sharon, D. Rosenblatt, and A. A. Friesem, *Opt. Commun.* **145**, 291 (1998).
13. D. Wawro, S. Tibuleac, R. Magnusson, and H. Liu, *Proc. SPIE* **3911**, 86 (2000).
14. B. Cunningham, P. Li, B. Lin, and J. Pepper, *Sens. Actuators B* **81**, 316 (2002).
15. M. A. Cooper, *Nat. Rev. Drug Discovery* **1**, 515 (2002).
16. R. Magnusson and S. S. Want, *Appl. Phys. Lett.* **61**, 1022 (1992).
17. S. Peng and G. Morris, *Opt. Lett.* **21**, 549 (1996).
18. V. V. Meriakri, I. P. Nikitin, and M. P. Parkhomenko, *Int. J. Infrared Millimeter Waves* **17**, 1769 (1996).
19. R. Magnusson, S. S. Wang, T. D. Black, and A. Sohn, *IEEE Trans. Antennas Propag.* **42**, 567 (1994).
20. P. S. Priambodo, T. A. Maldonado, and R. Magnusson, *Appl. Phys. Lett.* **83**, 3248 (2003).
21. R. Magnusson and Y. Ding, *IEEE Photon. Technol. Lett.* **18**, 1479 (2006).
22. R. Magnusson and M. Shokoh-Saremi, *Opt. Express* **15**, 10903 (2007).
23. F. Yang, G. Yen, G. Rasigade, J. A. N. T. Soares, and B. T. Cunningham, *Appl. Phys. Lett.* **92**, 091115 (2008).
24. F. Yang, G. Yen, and B. T. Cunningham, *Appl. Phys. Lett.* **90**, 261109 (2007).
25. A. S. P. Chang, K. J. Morton, P. F. Hua, T. Murphy, S. Y. Wei, and W. Chou, *IEEE Photon. Technol. Lett.* **19**, 1457 (2007).
26. M. Nevriere, R. Petit, and M. Cadilhac, *Opt. Commun.* **9**, 48 (1973).
27. I. Abdulhalim, *J. Opt. A: Pure Appl. Opt.* **1**, 646 (1999).
28. I. Abdulhalim, *Proc. SPIE* **6135**, 179 (2006).
29. I. Abdulhalim, in *Optical Waveguide Sensing and Imaging, NATO Science for Peace and Security Series*, W. J. Bock, I. Gannot, and S. Tanev, (eds.) (Springer, New York, 2008).
30. J. Li, S. T. Wu, S. Brugioni, R. Meucci, and S. Faetti, *J. Appl. Phys.* **97**, 073501 (2005).
31. A. Lahav, M. Auslender, and I. Abdulhalim, *Opt. Lett.* **33**, 2539 (2008).
32. I. C. Khoo and S. T. Wu, in *Optics and Nonlinear Optics of Liquid Crystals* (World Scientific, Singapore, 1993).